Refinement of the Hounsfield look-up table by retrospective application of patient-specific direct proton stopping-power prediction from dual-energy CT

Wohlfahrt, P.; Möhler, C.; Enghardt, W.; Krause, M.; Kunath, D.; Menkel, S.; Troost, E. G. C.; Greilich, S.; Richter, C.;

Originally published:

February 2020

Medical Physics 47(2020)4, 1796-1806

DOI: https://doi.org/10.1002/mp.14085

TITLE: Refinement of the Hounsfield look-up table by retrospective application of patient-specific direct proton stopping-power prediction from dual-energy CT

SHORTENED RUNNING TITLE: DECT-based HLUT refinement using DirectSPR

Authors: Patrick Wohlfahrt[*,†,1], Christian Möhler[‡,§], Wolfgang Enghardt[*,†,‖,¶], Mechthild Krause[*,†,‖,¶,#], Daniela Kunath[‖], Stefan Menkel[‖], Esther G. C. Troost[*,†,‖,¶,#], Steffen Greilich[‡,§], Christian Richter[*,†,‖,¶]

Institutions:

[*] OncoRay - National Center for Radiation Research in Oncology, Faculty of Medicine and University Hospital Carl Gustav Carus, Technische Universität Dresden, Helmholtz-Zentrum Dresden-Rossendorf, Dresden, Germany

[†] Helmholtz-Zentrum Dresden-Rossendorf, Institute of Radiooncology - OncoRay, Dresden, Germany

[‡] German Cancer Research Center (DKFZ), Heidelberg, Germany

[§] National Center for Radiation Research in Oncology (NCRO), Heidelberg Institute for Radiation Oncology (HIRO), Heidelberg, Germany

[‖] Department of Radiotherapy and Radiation Oncology, Faculty of Medicine and University Hospital Carl Gustav Carus, Technische Universität Dresden, Dresden, Germany

[¶] German Cancer Consortium (DKTK), Partner Site Dresden, Germany

[#] National Center for Tumor Diseases (NCT), Partner Site Dresden, Germany: German Cancer Research Center (DKFZ), Heidelberg, Germany; Faculty of Medicine and University Hospital Carl Gustav Carus, Technische Universität Dresden, Dresden, Germany, and; Helmholtz Association / Helmholtz-Zentrum Dresden-Rossendorf, Dresden, Germany

[1] now with Massachusetts General Hospital and Harvard Medical School, Department of Radiation Oncology, Boston, USA

Corresponding author: Patrick Wohlfahrt, PhD, Massachusetts General Hospital and Harvard Medical School, Department of Radiation Oncology, 125 Nashua ST, Boston, MA 02114, USA, E-mail: Patrick.Wohlfahrt@OncoRay.de

ABSTRACT:

Background and Purpose:

Proton treatment planning relies on an accurate determination of stopping-power ratio (SPR) from x-ray computed tomography (CT). A refinement of the heuristic CT-based SPR prediction using a state-of-the-art Hounsfield look-up table (HLUT) is proposed, which incorporates patient SPR information obtained from dual-energy CT (DECT) in a retrospective patient-cohort analysis.

Material and Methods:

SPR datasets of 25 brain-tumor, 25 prostate-cancer and three non-small cell lung-cancer (NSCLC) patients were calculated from clinical DECT scans with the comprehensively validated DirectSPR approach. Based on the median frequency distribution of voxelwise correlations between CT number and SPR within the irradiated volume, a piecewise linear function was specified (DirectSPR-based adapted HLUT). Differences in dose distribution and proton range were assessed for the non-adapted and adapted HLUT in comparison to the DirectSPR method, which has been shown to be an accurate and reliable SPR estimation method.

Results:

The application of the DirectSPR-based adapted HLUT instead of the non-adapted one reduced systematic proton range differences from 1.2% (1.1 mm) to -0.1% (0.0 mm) for brain-tumor patients, 1.7% (4.1 mm) to 0.2% (0.5 mm) for prostate-cancer patients and 2.0% (2.9 mm) to -0.1% (0.0 mm) for NSCLC patients. Due to the large intra- and inter-patient tissue variability, range differences to DirectSPR larger than 1% remained for the adapted HLUT.

Conclusions:

The incorporation of patient-specific correlations between CT number and SPR, derived from a retrospective application of DirectSPR to a broad patient cohort, improves the SPR accuracy of the current state-of-the-art HLUT approach. The DirectSPR-based adapted HLUT has been clinically implemented at the University Proton Therapy Dresden (Dresden, Germany) in 2017. This already facilitates the benefits of an improved DECT-based tissue differentiation within clinical routine without changing the general approach for range prediction (HLUT) and represents a further step towards full integration of the DECT-based DirectSPR method for treatment planning in proton therapy.

KEYWORDS:

dual-energy CT, proton stopping power, Hounsfield look-up table, proton therapy, proton range prediction, clinical translation

MANUSCRIPT:

Introduction

Imaging in radiation oncology steadily gains importance for treatment decision, tumor staging and delineation as well as accurate radiation treatment planning[1]. In particular proton and ion-beam therapy rely on precise and accurate computed tomography (CT) scans of patients to fully exploit the physical advantage of particle beams aiming for an improved clinical outcome and sparing of healthy tissue[2–5]. One substantial component of uncertainty arises from the current state-of-the-art conversion of CT number to stopping-power ratio (SPR) using a generic Hounsfield look-up table (HLUT), which shows a large variety between proton therapy centers[6]. A recent yet unpublished study within the European Particle Therapy Network (EPTN) revealed an inter-center variation in HLUT-based range prediction of 2.5% for targets in the head and pelvic region as determined in a phantom study. To account for the uncertainty of a generic HLUT for range prediction, considerable safety margins in beam direction are applied directly or indirectly (e.g., with robust optimization techniques), which finally result in a higher dose to healthy tissue close to the target[7–11].

While the acquisition of dual-energy CT (DECT) scans with their ability for an improved material differentiation is already very common for radiological purposes[12], its routine application in radiotherapy is still scarce[13, 14]. For the first time, proton treatment planning was routinely performed on DECT-derived pseudo-monoenergetic CT (MonoCT) datasets at the University Proton Therapy Dresden (UPTD) in 2015 still using a HLUT as CT-number-to-SPR conversion[15]. Noteworthy, patient-specific approaches for direct SPR prediction from DECT (DirectSPR) are very promising to reduce the CT-related range uncertainty and associated safety margins[16–18]. In comparison to the state-of-the-art HLUT approach, the reliability and superior accuracy of the DirectSPR method was recently demonstrated in high-precision experimental studies on different complexity levels arising in humans (Figure 1): (A) various homogeneous[19, 20] and heterogeneous biological tissue samples[21] to closely model

human tissue composition as well as (B) an anthropomorphic head phantom of known three-dimensional SPR distribution to simulate typical heterogeneities in patients[22]. Furthermore, retrospective patient-cohort analyses including brain-, prostate- and lung-tumor cases treated with proton therapy showed systematic range differences up to 2.3% on average between the HLUT and DirectSPR approach and highlighted the clinical relevance of accurate SPR prediction[23, 24]. These deviations are very likely induced by tissue compositions and tissue distributions differing from HLUT calibration conditions[25].

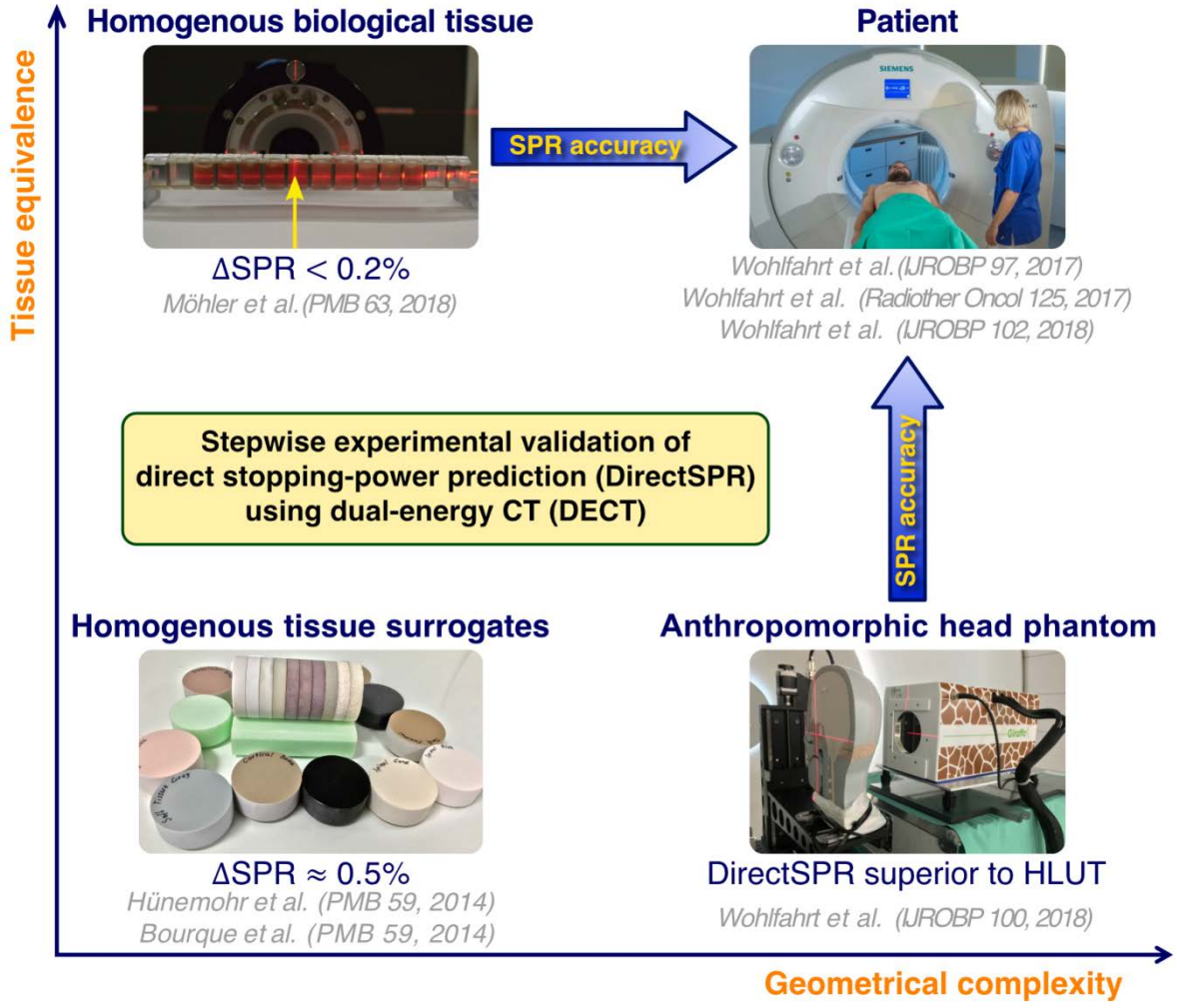

Figure 1: Experimental validation procedure to assess the accuracy (mean absolute error) of stopping-power ratio (SPR) derived from DECT using DirectSPR by separating two complexity levels arising in humans – the influence of tissue composition (y axis) and geometrical heterogeneities (x axis). The validation experiments reached an overall measurement uncertainty within 0.3% in SPR and 1 mm in range[19, 22]. The clinical relevance of patient-specific DirectSPR-based SPR prediction compared with the current state-of-the-art Hounsfield look-up table (HLUT) approach was demonstrated in patient-cohort analyses[15, 23, 24]. Adapted from [26].

To overcome the uncertainty in heuristic conversion of x-ray attenuation to proton stopping power, proton radiography or the so-called range probing were suggested for a patient-specific adaptation of the clinical HLUT prior to treatment[27–31]. Thus far, both techniques have not efficiently been integrated in a clinical workflow and as long as they are not part of standard clinical care, their application might also be subject to inspection within the radiation protection law and need an ethics approval prior to patient application due to the small additional radiation dose.

In this study, we propose the use of DECT-based SPR information, retrospectively obtained by the DirectSPR approach, to refine a clinical HLUT and thus benefit from an improved SPR accuracy achievable with DECT in current proton treatment planning without changing the general approach of range prediction (HLUT). This can be seen as conservative option for introducing DirectSPR information in range prediction. The refined HLUT already considers the respective tissue composition and distribution as well as the specific CT-number-to-SPR conversion in patients. DECT scans of more than 50 patients treated with proton therapy were retrospectively evaluated to assess the clinical applicability and performance of a DirectSPR-based HLUT refinement compared to the patient-specific DirectSPR method.

Material and Methods

DECT acquisition and image post-processing

Dual-spiral DECT scans (two consecutive CT scans of 80 and 140 kVp, respectively) have been acquired for routine proton treatment planning and during the course of treatment at a single-source CT scanner SOMATOM Definition AS (Siemens Healthineers, Forchheim, Germany)[23, 24]. To reduce image noise, the iterative reconstruction kernel Q34f/5 (SAFIRE at maximal strength) was applied for DECT image reconstruction with $1\times1\times2$ mm^3 voxel spacing. This kernel also contains an iterative beam hardening correction for bone to improve the CT number stability between several body regions and patient sizes[26].

MonoCT datasets of 79 keV and 170 keV were obtained from DECT scans using the module SYNGO.CT DE MONOENERGETIC PLUS of the image post-processing environment SYNGO.VIA (Siemens Healthineers, Forchheim, Germany). According to an in-house CT scanner characterization for the DECT scan protocol applied clinically[15], the 170 keV MonoCT dataset served as proxy for an accurate image-based assessment of relative electron density (RED)[32] and the 79 keV MonoCT dataset reveals a similar effective x-ray attenuation as the 140 kVp CT scan. Both DECT-derived image datasets were used to calculate the SPR with the DirectSPR approach referred to as RhoSigma[18]. According to the Bethe equation[33], a second factor beyond RED, the relative stopping number, needs to be determined for SPR prediction. For this purpose, the linear photon attenuation coefficient of the 79 keV MonoCT was divided by the electron density derived from the RED dataset to obtain the relative photon attenuation cross section (RCS). The relative stopping number was then empirically derived from RCS and multiplied with RED for voxelwise SPR calculation. Further details on the implementation of DirectSPR are explicitly described in previous publications[22, 23].

Patient cohort

In total, 25 brain-tumor and 25 prostate-cancer patients as well as three patients with advanced stage non-small cell lung cancer (NSCLC), treated in the clinical trial PRONTOX[34], were selected to consider different tumor entities, body regions and patient ages (2-84a). According to the routine clinical workflow[15], a passively scattered proton treatment plan was generated for each patient on the 79 keV MonoCT dataset with the clinical HLUT using the treatment planning system XiO (Elekta AB, Stockholm, Sweden) and a $1\times1\times1$ mm^3 dose calculation grid.

For the dual-spiral time-resolved DECT (4D-DECT) scans acquired for NSCLC cases, the time-averaged 79 keV MonoCT dataset was used for dose calculation. The number of

treatment fields varied between the cohorts: two for prostate-cancer (90°/270°), three for NSCLC and 2-5 for brain-tumor cases.

The retrospective evaluation of patient data was approved by the local ethics committee (EK535122015).

DirectSPR-based HLUT refinement

To incorporate patient tissue properties and their distribution in the HLUT specification, the frequency distribution of voxelwise correlations between CT numbers H, obtained from 79 keV MonoCT datasets, and DirectSPR-derived SPRs was determined. All CT voxels within the irradiated volume confined by the 20% isodose of the clinical treatment plan were considered including patient-specific immobilization devices, such as thermoplastic mask, vacuum cushion and endorectal balloon. Based on the DECT-derived frequency distribution representative for patient treatments and information on tabulated human tissues[35], the Hounsfield scale was categorized in low-density ($-900\ \text{HU} \leq H \leq -150\ \text{HU}$), adipose ($-120\ \text{HU} \leq H \leq -70\ \text{HU}$), muscle/brain ($-20\ \text{HU} \leq H \leq 70\ \text{HU}$) and bone tissue ($200\ \text{HU} \leq H \leq 1350\ \text{HU}$). For each tissue category, the median SPR was determined for every CT number from the frequency distribution and then a weighted linear regression was aligned to the median SPR distribution considering the relative occurrence of each CT number as weight for the least square optimization. Finally, intermediate intervals were linearly connected to create a stepwise linear and continuous HLUT.

This DirectSPR-based HLUT refinement was performed separately for all three patient cohorts. In addition, the cohort-specific frequency distributions were normalized regarding the respective number of patients and then merged to generate a collectively adapted HLUT, optimized for the combination of all sub-cohorts.

To assess the robustness of the HLUT adaptation, a leave-one-out cross validation was performed for each patient cohort. The coefficient of variation (CoV) for the slope and

intercept of the linear regression performed for the four tissue categories was determined to quantify the dependence on patient datasets.

Assessment of SPR and range deviations

The mean SPR difference ($\Delta\mathrm{SPR} = \mathrm{SPR}_{\mathrm{HLUT}} - \mathrm{SPR}_{\mathrm{DirectSPR}}$) between the DirectSPR approach and each HLUT (non-adapted clinical, cohort-specifically and collectively adapted HLUT) was determined within the irradiated volume of each patient.

To assess the impact of several CT-number-to-SPR conversion methods on the dose distribution, the clinical proton treatment plan was recalculated (a) on the DirectSPR-based SPR dataset, serving as the best possible assumption of the ground truth, (b) as well as on the 79 keV MonoCT dataset using the collectively adapted HLUT, containing information from all sub-cohorts. Relative dose difference maps (normalized to prescribed dose) and water-equivalent range shifts ($\Delta\mathrm{R} = \mathrm{R}_{\mathrm{DirectSPR}} - \mathrm{R}_{\mathrm{HLUT}}$) between the DirectSPR approach and each HLUT were evaluated for the two main treatment fields of each patient. An in-house implemented ray-tracing method was applied to extract depth-dose curves with 1 mm spacing orthogonal to the beam direction[23]. The proton range was defined as distal range at 80% of reference dose.

Results

DirectSPR-based HLUT refinement

The HLUTs before and after refinement based on DirectSPR differed (Figure 2). For the non-adapted clinical HLUT, systematic SPR deviations in the muscle/brain region ($20\ \mathrm{HU} \leq H \leq 60\ \mathrm{HU}$) as well as different slopes for low-density ($H \leq -150\ \mathrm{HU}$) and bone tissues ($H \geq 200\ \mathrm{HU}$) were found in comparison to the SPR distribution determined by the DirectSPR approach (Figure 2B). These systematic differences were substantially reduced by refining the HLUT using the median DirectSPR-based SPR distribution (Figure 3A). For the three patient

cohorts, the mean SPR difference between the DirectSPR method and HLUT adapted as a whole or per cohort was within 0.2%.

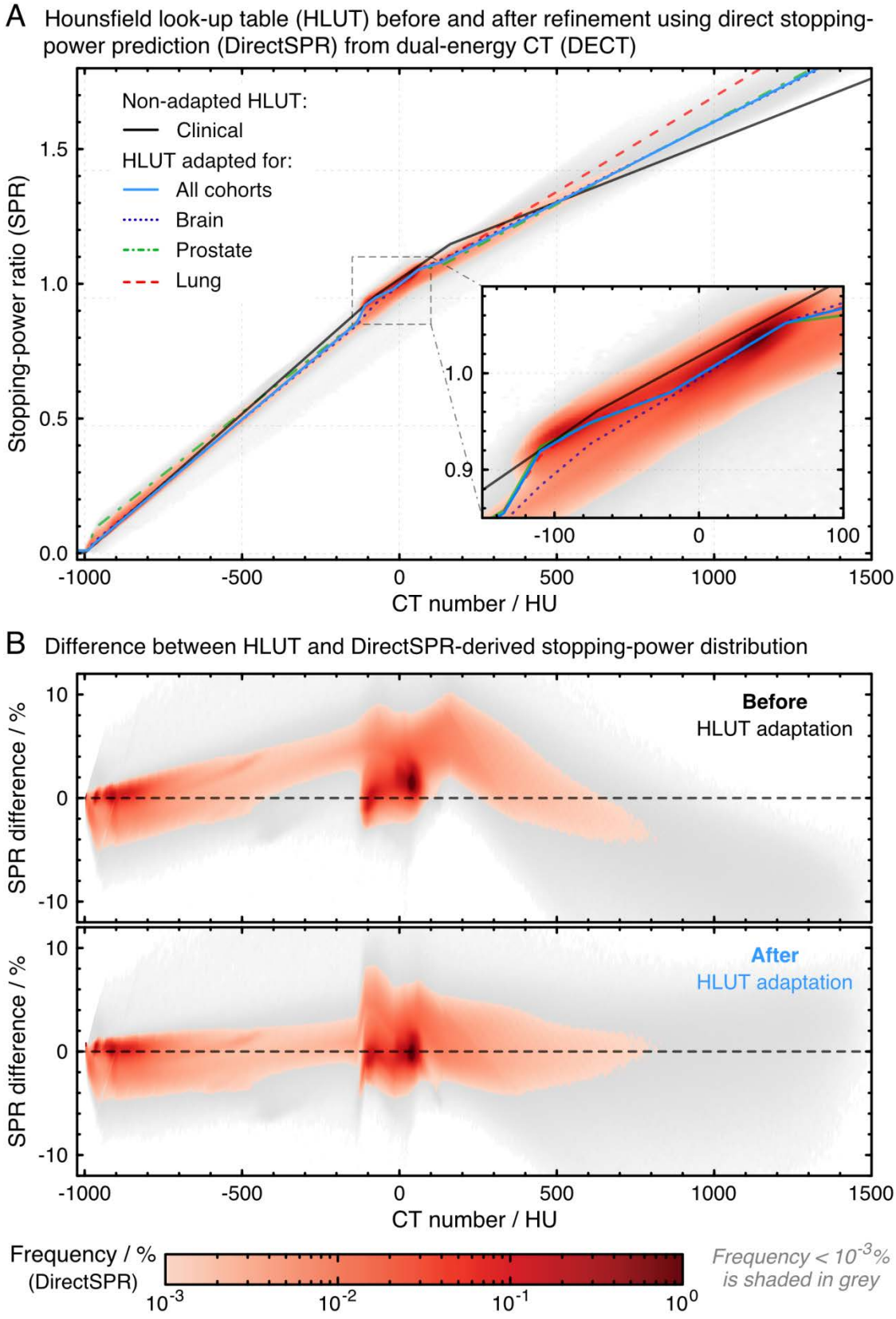

Figure 2: Frequency distribution of (A) DirectSPR-derived SPR for the collective cohort overlaid with the non-adapted clinical as well as cohort-specifically and collectively adapted HLUT, and (B) differences between SPR derived by DirectSPR and the HLUT before and after collective refinement. CT numbers were determined from a DECT-derived 79 keV pseudo-monoenergetic CT dataset.

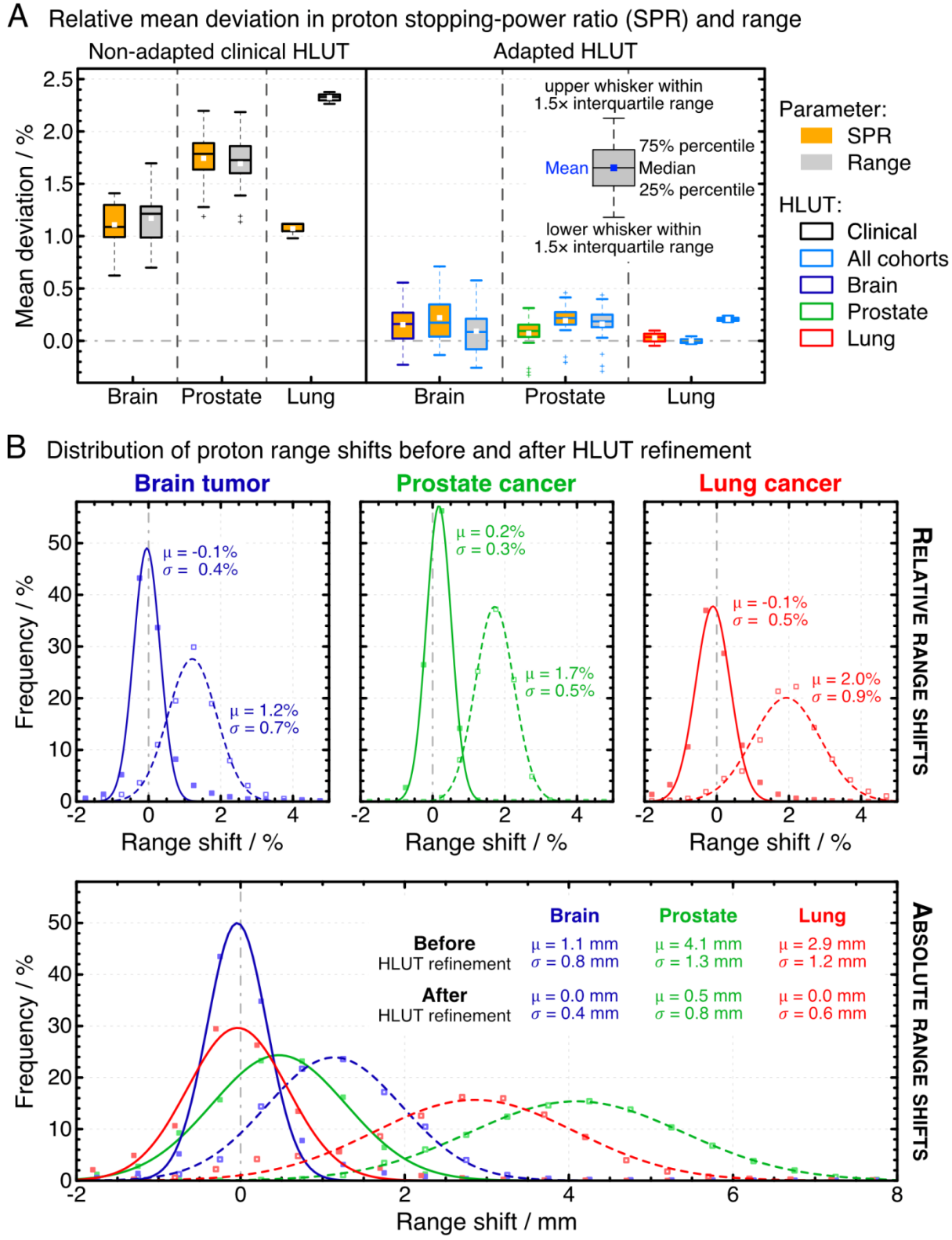

Figure 3: (A) Boxplot of mean SPR deviations and water-equivalent range shifts between the direct SPR prediction from dual-energy CT (DirectSPR) and the non-adapted clinical Hounsfield look-up table (HLUT) as well as the HLUT adapted for each cohort separately or altogether. (B) Distribution of range shifts before (dashed line) and after (solid line) collective HLUT refinement. A Gaussian distribution was fitted to the respective data (shown as squares).

Cohort-specific DirectSPR-based HLUT refinement

The HLUTs adapted separately for each cohort differed in several tissue categories (Figure 2A). Since air only rarely occurs in treatment fields of prostate-cancer patients, the slope for the low-density tissue region ($H \leq -150$ HU) was mainly defined by mixtures of air and soft tissues at the body surface or rectal wall. Treatment plans of prostate-cancer cases are highly standardized using opposing beams from 90° and 270°, which translated into a very robust determination of the intercept (CoV < 0.1%) and slope (CoV = 0.6% for adipose and CoV ≤ 0.1% for the other three categories). The slightly larger slope variation within the adipose segment can be explained by differences in the amount of adipose tissues between patients.

In NSCLC cases, the slope of the HLUT line segment for bones ($H \geq 200$ HU) was aligned to the SPR distribution of low-density bone structures within ribs, because bones of high density (e.g. cortical bone) sparsely occur in this body region. This led to an increased slope in this CT number region compared with the other two cohorts. Due to the large variation in tumor position and thus beam angle selection as well as the limited number of lung-cancer cases included, the tissue distribution in beam direction varies considerably. This is also shown in the robustness of the intercept (CoV ≤ 0.6%) and slope (CoV of 0.4%, 10.0%, 2.6% and 3.5% for the low-density, adipose, muscle and bone tissue category, respectively).

In contrast, the HLUT adapted for brain-tumor patients showed a different behavior within the adipose tissue category (-120 HU $\leq H \leq -70$ HU) than the other two cohorts. Since brain tissue is the most common tissue species in beam direction, the SPR distribution in the adipose tissue category is a superposition of adipose tissues as well as mixtures of soft tissues (mainly brain and muscle, 20 HU $\leq H \leq 60$ HU) and air cavities, which result in a smaller

SPR than adipose tissues for the same CT number. The larger variability for this tissue category is also expressed by a less robust intercept (CoV = 0.3%) and slope (CoV = 3.0%) compared with the robustness of the intercept (CoV < 0.1%) and slope (CoV of 0.1%, 0.7%, 0.2% for the low-density, brain/muscle and bone segment, respectively) in the other three tissue categories.

Importantly, despite all these differences, a cohort-specific HLUT adaptation resulted only in a slight additional reduction of SPR deviations of approximately 0.1% on average compared with the HLUT refined for all patients combined irrespective of the tumor entity (Figure 3A). Due to the combination of different body regions (abdomen/pelvis, thorax, head), the entire width of the Hounsfield scale could be adequately covered for a universal HLUT specification.

Dosimetric and proton range deviations

Since no clinically relevant improvement was determined on SPR level using a cohort-specific HLUT, compared to the HLUT refined for all cohorts together, only the collectively refined HLUT was used for dose comparisons and range evaluations. In Figure 4, an exemplary dose distribution for a representative treatment field of a prostate-cancer patient is shown using the DirectSPR approach as well as non-adapted clinical and adapted HLUT as CT-number-to-SPR conversion. Dose differences distal and proximal to the target volume were almost removed using the DirectSPR-based adapted HLUT instead of the non-adapted one. For an exemplary depth-dose curve, the water-equivalent range shift could thus be reduced from 5.1 mm (2.2%) to 1.2 mm (0.5%). Considering all depth-dose curves evaluated for each treatment field of all patients (on average 5000 per field), the mean relative water-equivalent range shift ± standard deviation between patients decreased from (1.17 ± 0.22)% to (0.09 ± 0.20)% for brain-tumor patients, (1.69 ± 0.24)% to (0.16 ± 0.17)% for prostate-cancer patients and (2.32 ± 0.05)% to (0.21 ± 0.02)% for NSCLC patients (Figure 3A and 3B).

Consequently, the mean relative (absolute) range shift after HLUT refinement was within ±0.2% (0.5 mm) for all cohorts. The remaining intra-patient variation in range shifts as shown in Figure 5 highlights the case dependency and ambiguity of the HLUT approach.

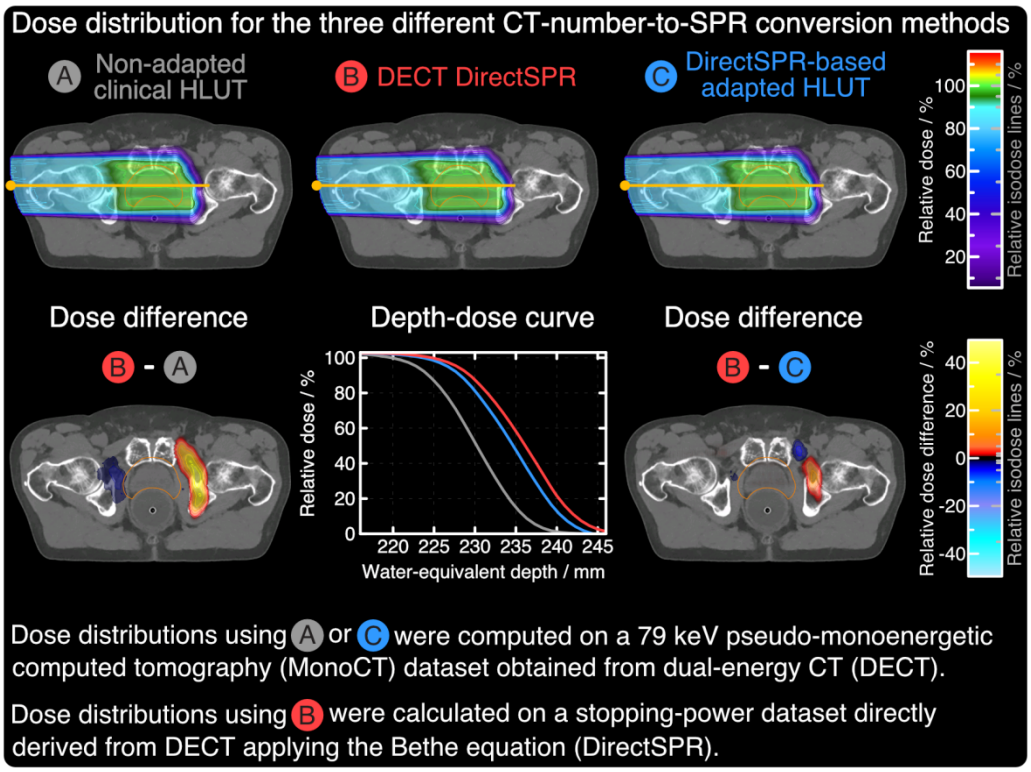

Figure 4: Exemplary dose distribution and depth-dose curve (extracted along the yellow line shown in the dose distributions of the top row) of a single proton treatment field of a representative prostate-cancer patient for three different conversions from CT number to stopping-power ratio (SPR) – non-adapted clinical (A) and adapted (C) Hounsfield look-up table (HLUT) as well as DECT-based DirectSPR approach (B).

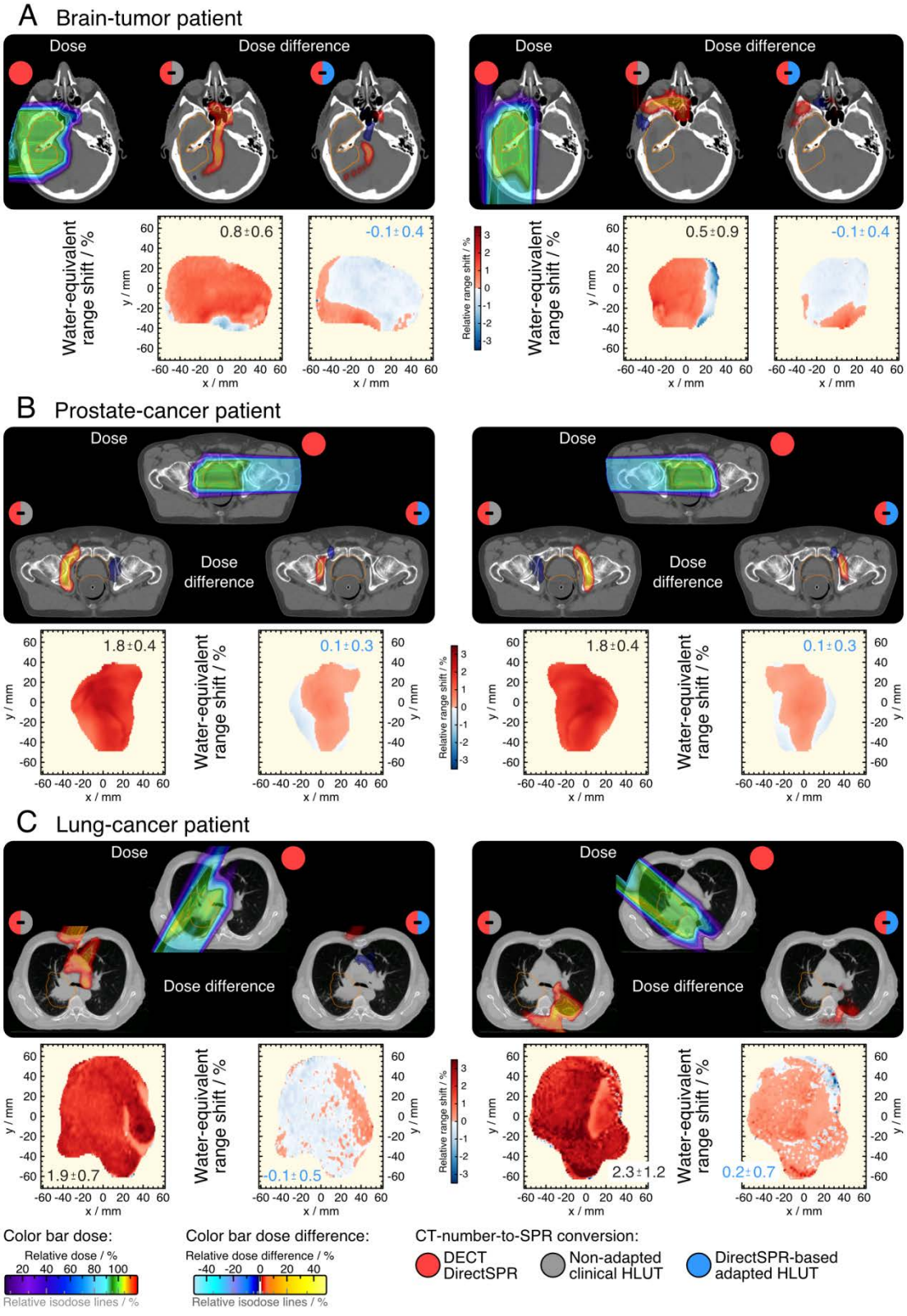

Figure 5: Dose distribution and difference between direct stopping-power prediction (DirectSPR) from dual-energy CT (DECT) and non-adapted clinical or adapted Hounsfield look-up table (HLUT) for two selected proton treatment fields of three patient cases. For the respective treatment field, relative water-equivalent range shifts in beam direction are illustrated in beam's eye view (IEC gantry coordinate system) with the corresponding (mean ± standard deviation).

Discussion

This retrospective patient-cohort analysis demonstrates that the current state-of-the-art CT-number-to-SPR conversion in proton treatment planning using a HLUT can be refined by tissue information derived from dual-energy CT. Systematic SPR and range deviations between the DECT-based DirectSPR and HLUT approach were substantially reduced below 0.2% (0.5 mm) on average for each patient cohort. Incorporating tissue compositions and distributions directly derived from patients counteract one major drawback of the current HLUT approach and its calibration, namely the limited tissue equivalency of surrogate materials regarding x-ray and proton interactions[25]. Furthermore, SPR information obtained by DirectSPR provides guidance to select sampling points and specify the course of a HLUT[6] depending on the respective tissue occurrence. Hence, a HLUT specification following the clinical standards considering only prior knowledge of tissue surrogates and tabulated human tissues (no tissue distribution and tissue mixtures) can lead to clinically relevant deviations, which are rather challenging if not impossible to avoid without including additional patient-specific information as determined by DECT, for instance.

Since the proposed HLUT refinement is not altering the current state-of-the-art workflow in proton treatment planning, it allows for an immediate clinical application. This opens up the possibility to already benefit from an improved SPR accuracy achievable with DECT without the widespread availability of DirectSPR as medical product. Even proton facilities without DECT scanners yet can gain insights from the presented patient-cohort analysis to adapt the course of their HLUT considering the tissue distribution within patients. It might be possible for some institutions to use the refined HLUT presented here (Table 1), if comparable CT scan settings (in particular tube voltage of 140 kVp, reconstruction kernel D34/Q34 and slice collimation of 1.2 mm) and hardware are available. However, measurements for CT quality assurance are strongly recommended before clinical application to ensure that similar CT numbers are determined for tissue surrogates (provided on request for respective scan setup).

Since the material-specific CT numbers for two CT scanners of the same model available at UPTD (used for patient simulation and as in-room CT scanner on rails) showed only minor differences, the same HLUT is applied in clinical routine.

The DirectSPR-based HLUT refinement represents another important step towards a safe and reliable full routine application of DECT in proton treatment planning, which is in accordance with the current methodology. In contrast, for a routine prospective clinical use of patient-specific DECT-based SPR prediction, an approved medical product with dedicated CT scanner calibration, thorough validation and full integration in clinical workflow is needed. However, this is not yet available.

In 2017, we adapted the HLUT for treatment planning at UPTD for cerebral and pelvic tumor patients considering DirectSPR-derived SPR information of the brain-tumor and prostate-cancer cohorts presented in this publication. The resulting HLUT is similar to the collectively adapted HLUT (Figure 6, Table 1). With this clinical implementation, the DirectSPR approach was for the first time clinically used for CT-based range prediction. Even though it was an indirect application, evidence of its applicability, accuracy and validity was an obligatory prerequisite for this decision. This could only be guaranteed by numerous experimental studies and retrospective patient analyses (Figure 1). An experimental verification with a measurement uncertainty smaller than 1%, which is needed to reliably demonstrate differences between CT-based SPR prediction approaches and their SPR accuracy, is very challenging and thus requires a coordinated optimization of CT scan settings and measurement setups considering the respective limitations in image acquisition and range measurements. Even small changes or deviations, such as change in setup between calibration and verification, the handling of inhomogeneities in tissue samples as well as spatial differences in range prediction (from the CT-derived SPR dataset directly, using raytracing or dose calculation with an analytical model or Monte Carlo simulation) and range measurement, can already lead to an unwanted measurement uncertainty larger than 1%.

Since these parameters often introduce a systematic uncertainty, which is comparable for several methods, relative differences between approaches are only slightly affected. However, since the imaging- and method-related uncertainty in SPR prediction can still lead to deviations in absolute proton range calculation, the clinically applied range uncertainty of 3.5% was not changed for the adapted HLUT, but this is expected to be feasible with the clinical introduction of DirectSPR. In future, the intended improvements in range prediction could be potentially directly validated by prompt-gamma measurements in patients considering the recent improvements in reproducibility and accuracy of geometrical positioning as well as software and hardware developments[36–39].

The DirectSPR approach applied in this study is a pure image-based algorithm, which does not consider the DECT information of each projection in the reconstruction of the 80/140 kVp DECT dataset. Hence, beam hardening can only be corrected for predefined materials, such as water and bone in this case, meaning that an uncertainty in CT number stability still remains[26]. An iterative method for the prediction of material properties based on x-ray projections of both CT acquisitions might even further reduce systematic effects of beam hardening and image noise on SPR estimation in future[40, 41].

The application of an HLUT for CT-number-to-SPR conversion is still limited in accuracy by its inherent ambiguity. A refined HLUT can reduce systematic range deviations on average, but cannot fully incorporate variations between patients and the intra-patient tissue variability[42]. Hence, range deviations larger than 0.5% or even 1.0% still occur for beam trajectories traversing tissues, which differ from the mean tissue distribution and thus hinder an ideal compensation of SPR under- and overestimation of various tissues (Figure 3B and 5). Since in particular the SPR distribution of bones clearly differs between patients (depending on the embedded calcium content), the course of the HLUT in the bone region might be ideally optimized separately for patients of different age[42]. Such an adaptation would further reduce range differences for individual patients, but this effect would be smaller than the

change in slope of the bone segment for the HLUT before and after refinement (Figure 6). Expectably, this intra- and inter-patient variability could be better accounted for using the DirectSPR approach directly[42].

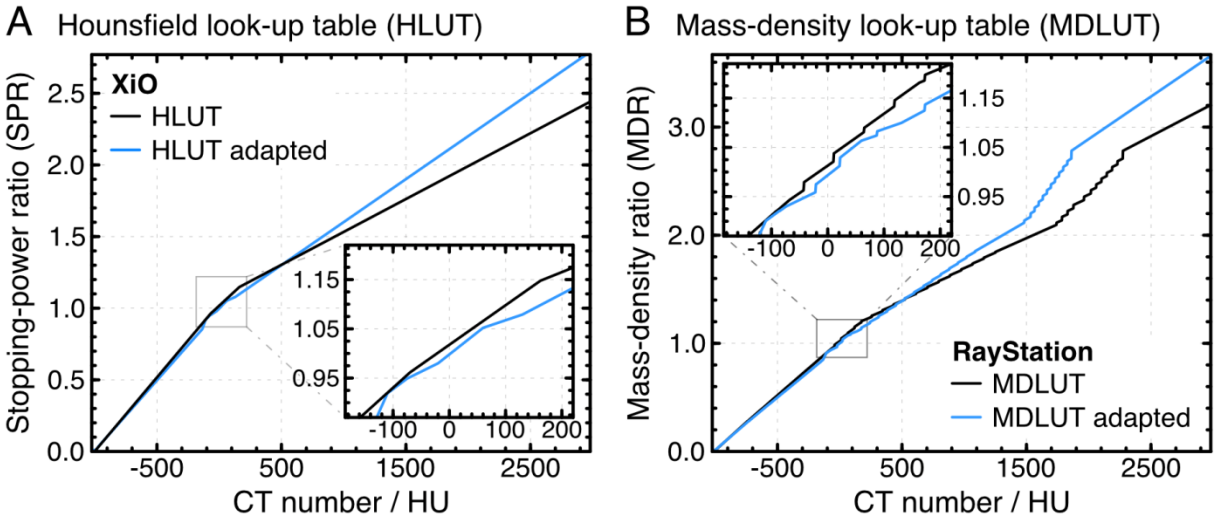

Figure 6: Conversion from CT number to (A) stopping-power ratio (SPR) and (B) mass-density ratio (MDR) relative to water before and after HLUT refinement as clinically implemented in the treatment planning system XiO and RayStation at the University Proton Therapy Dresden, respectively.

Table 1: Clinical conversion from CT number to stopping-power ratio (SPR) before and after refinement of the Hounsfield look-up table (HLUT). The conversions from CT number to mass-density ratio (MDR) for the treatment planning system RayStation are provided as supplementary material.

Clinical CT-number-to-SPR conversion	
Before HLUT refinement	
CT number / HU	-1024; -1000; -70; 162; 3071
SPR	0.001; 0.001; 0.961; 1.148; 2.483
After HLUT refinement	
CT number / HU	-1024; -1000; -970; -135; -110; -75; -20; 60; 130; 3071
SPR	0.001; 0.001; 0.035; 0.855; 0.919; 0.949; 0.980; 1.052; 1.079; 2.844

The adapted HLUT can also contribute to partly overcome some of the current technical limitations of DECT. Since dual-source CT scanners only provide DECT information in a

limited field of view (FOV) of up to 35 cm, a HLUT refined by DirectSPR could be used for SPR prediction in the case a larger FOV is needed for treatment planning as in the abdominal or pelvic region. Furthermore, the acquisition of time-resolved (4D) single-energy CT (SECT) scans is still mandatory for moving targets, because 4D-DECT is nowadays not clinically available and part of ongoing research. Hence, an adapted HLUT would instantly provide a clearly improved SPR accuracy for these cases.

In contrast to the brain-tumor and prostate-cancer patient cohorts, the mean SPR deviation (1.1%) considerably differed from the mean water-equivalent range shift (2.3%) for NSCLC patients before HLUT refinement (Figure 3A). This is most probably induced by the influence of severe tissue inhomogeneities within the irradiated volume. Tissue inhomogeneities lead to a higher variability in multiple Coulomb scattering for different proton trajectories, which is considered in dose calculation and thus range shifts derived from dose distributions, but of cause do not influence the voxelwise SPR prediction.

The minor improvement (0.1%) in accuracy of a HLUT adapted separately for each patient cohort can be neglected with respect to other uncertainties in dose calculation. Furthermore, the use of a single HLUT would facilitate the clinical workflow and prevent possible errors due to an incorrect HLUT assignment.

Since the overall dose distribution of each treatment field was analyzed, the results obtained for double scattering in this study can be also translated to treatment planning with pencil beam scanning. The impact of beam model and dose calculation algorithm (pencil beam vs. Monte Carlo approach) on relative range shifts is expected to be minor and would not change the conclusions drawn here. Future studies should include more patients and different tumor sites (within the head-and-neck or abdominal region) to assess potential differences in HLUT specification.

It should be also noted for the sake of completeness that dual-spiral DECT acquisition is prone to patient motion (e.g., swallowing or breathing) during the two consecutive CT scans

resulting in a different anatomical representation. This uncertainty can be restricted by a robust and reproducible patient immobilization and a time-resolved CT acquisition if required. Remaining uncorrelated motion effects can be efficiently corrected by a deformable image registration during image post-processing[23, 24].

Conclusions

Patient-specific tissue information derived from dual-energy CT with the DirectSPR approach can be considered to refine the current state-of-the-art heuristic CT-number-to-SPR conversion in particle therapy. After HLUT adaptation, average SPR and range differences between the superior and more accurate direct DECT-based SPR prediction and a HLUT were within 0.2%. The DirectSPR-based adapted HLUT was clinically implemented, which already allows for an immediate benefit from additional information derived from DECT without altering the current clinical methodology and workflow.

REFERENCES

[1] M. Baumann, M. Krause, J. Overgaard, *et al.*, Radiation Oncology in the Era of Precision Medicine, Nat. Rev. Cancer **16**(4), 234–249 (2016).

[2] M. Goitein, Calculation of the Uncertainty in the Dose Delivered During Radiation Therapy, Med. Phys. **12**(5), 608–612 (1985).

[3] H. Paganetti, Range Uncertainties in Proton Therapy and the Role of Monte Carlo Simulations, Phys. Med. Biol. **57**(11), R99--------R117 (2012).

[4] A.-C. Knopf and A.J. Lomax, In Vivo Proton Range Verification: A Review, Phys. Med. Biol. **58**(15), R131--------R160 (2013).

[5] E. Dinges, N. Felderman, S. McGuire, *et al.*, Bone Marrow Sparing in Intensity Modulated Proton Therapy for Cervical Cancer: Efficacy and Robustness Under Range and Setup Uncertainties, Radiother. Oncol. **115**(3), 373–378 (2015).

[6] V.T. Taasti, C. Bäumer, C. V Dahlgren, *et al.*, Inter-Centre Variability of CT-Based Stopping-Power Prediction in Particle Therapy: Survey-Based Evaluation, Phys. Imaging Radiat. Oncol. **6**(April), 25–30 (2018).

[7] G. Fattori, M. Riboldi, E. Scifoni, *et al.*, Dosimetric Effects of Residual Uncertainties in Carbon Ion Treatment of Head Chordoma, Radiother. Oncol. **113**(1), 66–71 (2014).

[8] H. Li, X. Zhang, P.C. Park, *et al.*, Robust Optimization in Intensity-Modulated Proton Therapy to Account for Anatomy Changes in Lung Cancer Patients, Radiother. Oncol. **114**(3), 367–372 (2015).

[9] S. van Der Voort, S. van De Water, Z. Perkó, B. Heijmen, D. Lathouwers, and M. Hoogeman, Robustness Recipes for Minimax Robust Optimization in Intensity Modulated Proton Therapy for Oropharyngeal Cancer Patients, Int. J. Radiat. Oncol. Biol. Phys. **95**(1), 163–170 (2016).

[10] K. Stützer, A. Lin, M.L. Kirk, and L. Lin, Superiority in Robustness of Multifield Optimization Over Single-Field Optimization for Pencil-Beam Proton Therapy for

Oropharynx Carcinoma: An Enhanced Robustness Analysis, Int. J. Radiat. Oncol. Biol. Phys. **99**(3), 738–749 (2017).

[11] M. Cubillos-Mesías, E.G.C. Troost, F. Lohaus, *et al.*, Including Anatomical Variations in Robust Optimization for Head and Neck Proton Therapy can Reduce the Need of Adaptation, Radiother. Oncol. **131**, 127–134 (2019).

[12] B. Krauss, Dual-Energy Computed Tomography, Radiol. Clin. North Am. **56**(4), 497–506 (2018).

[13] W. van Elmpt, G. Landry, M. Das, and F. Verhaegen, Dual Energy CT in Radiotherapy: Current Applications and Future Outlook, Radiother. Oncol. **119**(1), 137–144 (2016).

[14] P. Wohlfahrt and C. Richter, Status and Innovations in Pre-Treatment CT Imaging for Proton Therapy, Br. J. Radiol. **92**, 20190590 (2019).

[15] P. Wohlfahrt, C. Möhler, V. Hietschold, *et al.*, Clinical Implementation of Dual-Energy CT for Proton Treatment Planning on Pseudo-Monoenergetic CT Scans, Int. J. Radiat. Oncol. Biol. Phys. **97**(2), 427–434 (2017).

[16] N. Hünemohr, B. Krauss, C. Tremmel, B. Ackermann, O. Jäkel, and S. Greilich, Experimental Verification of Ion Stopping Power Prediction from Dual Energy CT Data in Tissue Surrogates, Phys. Med. Biol. **59**(1), 83–96 (2014).

[17] A.E. Bourque, J.-F. Carrier, and H. Bouchard, A Stoichiometric Calibration Method for Dual Energy Computed Tomography, Phys. Med. Biol. **59**(8), 2059–2088 (2014).

[18] C. Möhler, P. Wohlfahrt, C. Richter, and S. Greilich, Range Prediction for Tissue Mixtures Based on Dual-Energy CT, Phys. Med. Biol. **61**(11), N268--------N275 (2016).

[19] C. Möhler, T. Russ, P. Wohlfahrt, *et al.*, Experimental Verification of Stopping-Power Prediction from Single- and Dual-Energy Computed Tomography in Biological Tissues, Phys. Med. Biol. **63**(2), 25001 (2018).

[20] V.T. Taasti, G.J. Michalak, D.C. Hansen, *et al.*, Validation of Proton Stopping Power Ratio Estimation Based on Dual Energy CT Using Fresh Tissue Samples, Phys. Med. Biol. **63**(1), 15012 (2018).

[21] E. Bär, A. Lalonde, R. Zhang, *et al.*, Experimental Validation of two Dual-Energy CT Methods for Proton Therapy Using Heterogeneous Tissue Samples, Med. Phys. **45**(1), 48–59 (2018).

[22] P. Wohlfahrt, C. Möhler, C. Richter, and S. Greilich, Evaluation of Stopping-Power Prediction by Dual- and Single-Energy Computed Tomography in an Anthropomorphic Ground-Truth Phantom, Int. J. Radiat. Oncol. Biol. Phys. **100**(1), 244–253 (2018).

[23] P. Wohlfahrt, C. Möhler, K. Stützer, S. Greilich, and C. Richter, Dual-Energy CT Based Proton Range Prediction in Head and Pelvic Tumor Patients, Radiother. Oncol. **125**(3), 526–533 (2017).

[24] P. Wohlfahrt, E.G.C. Troost, C. Hofmann, C. Richter, and A. Jakobi, Clinical Feasibility of Single-Source Dual-spiral 4D Dual-Energy CT for Proton Treatment Planning Within the Thoracic Region, Int. J. Radiat. Oncol. Biol. Phys. **102**(4), 830–840 (2018).

[25] P. Wohlfahrt, C. Möhler, S. Greilich, and C. Richter, Comment on: Dosimetric Comparison of Stopping-Power Calibration with Dual-Energy CT and Single-Energy CT in Proton Therapy Treatment Planning [Med. Phys. 43(6), 2845-2854 (2016)], Med. Phys. **44**(10), 5533–5536 (2017).

[26] P. Wohlfahrt, Dual-Energy Computed Tomography for Accurate Stopping-Power Prediction in Proton Treatment Planning (TU Dresden, 2018).

[27] U. Schneider, P. Pemler, J. Besserer, E. Pedroni, A.J. Lomax, and B. Kaser-Hotz, Patient Specific Optimization of the Relation Between CT-Hounsfield Units and Proton Stopping Power with Proton Radiography, Med. Phys. **32**(1), 195–199 (2005).

[28] P.J. Doolan, M. Testa, G.C. Sharp, E.H. Bentefour, G. Royle, and H. Lu, Patient-

Specific Stopping Power Calibration for Proton Therapy Planning Based on Single-Detector Proton Radiography, Phys. Med. Biol. **60**(5), 1901–1917 (2015).

[29] P. Farace, R. Righetto, S. Deffet, *et al.*, Technical Note : A Direct Ray-Tracing Method to Compute Integral Depth Dose in Pencil Beam Proton Radiography with a Multilayer Ionization Chamber, Med. Phys. **43**(12), 6405–6412 (2016).

[30] C.-A. Collins-Fekete, S. Brousmiche, D.C. Hansen, L. Beaulieu, and J. Seco, Pre-Treatment Patient-Specific Stopping Power by Combining List-Mode Proton Radiography and X-Ray CT, Phys. Med. Biol. **62**(17), 6836–6852 (2017).

[31] N. Krah, V. Patera, S. Rit, A. Schiavi, and I. Rinaldi, Regularised Patient-Specific Stopping Power Calibration for Proton Therapy Planning Based on Proton Radiographic Images, Phys. Med. Biol. **64**(6), 65008 (2019).

[32] C. Möhler, P. Wohlfahrt, C. Richter, and S. Greilich, Methodological Accuracy of Image-Based Electron Density Assessment Using Dual-Energy Computed Tomography, Med. Phys. **44**(6), 2429–2437 (2017).

[33] H. Bethe, Zur Theorie des Durchgangs schneller Korpuskularstrahlen durch Materie, Ann. Phys. **397**(3), 325–400 (1930).

[34] S. Zschaeck, M. Simon, S. Löck, *et al.*, PRONTOX – Proton Therapy to Reduce Acute Normal Tissue Toxicity in Locally Advanced Non-Small-Cell Lung Carcinomas (NSCLC): Study Protocol for a Randomised Controlled Trial, Trials **17**(1), 543 (2016).

[35] H.Q. Woodard and D.R. White, The Composition of Body Tissues, Br. J. Radiol. **59**(708), 1209–1219 (1986).

[36] C. Richter, G. Pausch, S. Barczyk, *et al.*, First Clinical Application of a Prompt Gamma Based In Vivo Proton Range Verification System, Radiother. Oncol. **118**(2), 232–237 (2016).

[37] Y. Xie, E.H. Bentefour, G. Janssens, *et al.*, Prompt Gamma Imaging for In Vivo Range Verification of Pencil Beam Scanning Proton Therapy, Int. J. Radiat. Oncol. Biol.

Phys. **99**(1), 210–218 (2017).

[38] F. Hueso-González, M. Rabe, T.A. Ruggieri, T. Bortfeld, and J.M. Verburg, A Full-Scale Clinical Prototype for Proton Range Verification Using Prompt Gamma-Ray Spectroscopy, Phys. Med. Biol. **63**(18), 185019 (2018).

[39] J. Berthold, C. Khamfongkhruea, J. Petzoldt, *et al.*, Improved Accuracy of Prompt-Gamma-Based Range Verification System Enabling Validation of CT-Based Stopping-Power Prediction, in *Int. J. Part. Ther.*(2019).

[40] S. Zhang, D. Han, D.G. Politte, J.F. Williamson, and J.A. O'Sullivan, Impact of Joint Statistical Dual-Energy CT Reconstruction of Proton Stopping Power Images: Comparison to Image- and Sinogram-Domain Material Decomposition Approaches, Med. Phys. **45**(5), 2129–2142 (2018).

[41] S. Zhang, D. Han, J.F. Williamson, *et al.*, Experimental Implementation of a Joint Statistical Image Reconstruction Method for Proton Stopping Power Mapping from Dual-Energy CT Data, Med. Phys. **46**(1), 273–285 (2019).

[42] P. Wohlfahrt, C. Möhler, E.G.C. Troost, S. Greilich, and C. Richter, Dual-Energy Computed Tomography to Assess Intra- and Inter-Patient Tissue Variability in Proton Treatment Planning of Patients with Brain Tumor, Int. J. Radiat. Oncol. Biol. Phys. (2019).

FIGURE AND TABLE CAPTIONS

Figure 1: Experimental validation procedure to assess the accuracy (mean absolute error) of stopping-power ratio (SPR) derived from DECT using DirectSPR by separating two complexity levels arising in humans – the influence of tissue composition (y axis) and geometrical heterogeneities (x axis). The validation experiments reached an overall measurement uncertainty within 0.3% in SPR and 1 mm in range[19, 22]. The clinical relevance of patient-specific DirectSPR-based SPR prediction compared with the current state-of-the-art Hounsfield look-up table (HLUT) approach was demonstrated in patient-cohort analyses[15, 23, 24]. Adapted from [26].

Figure 2: Frequency distribution of (A) DirectSPR-derived SPR for the collective cohort overlaid with the non-adapted clinical as well as cohort-specifically and collectively adapted HLUT, and (B) differences between SPR derived by DirectSPR and the HLUT before and after collective refinement. CT numbers were determined from a DECT-derived 79 keV pseudo-monoenergetic CT dataset.

Figure 3: (A) Boxplot of mean SPR deviations and water-equivalent range shifts between the direct SPR prediction from dual-energy CT (DirectSPR) and the non-adapted clinical Hounsfield look-up table (HLUT) as well as the HLUT adapted for each cohort separately or altogether. (B) Distribution of range shifts before (dashed line) and after (solid line) collective HLUT refinement. A Gaussian distribution was fitted to the respective data (shown as squares).

Figure 4: Exemplary dose distribution and depth-dose curve (extracted along the yellow line shown in the dose distributions of the top row) of a single proton treatment field of a

representative prostate-cancer patient for three different conversions from CT number to stopping-power ratio (SPR) – non-adapted clinical (A) and adapted (C) Hounsfield look-up table (HLUT) as well as DECT-based DirectSPR approach (B).

Figure 5: Dose distribution and difference between direct stopping-power prediction (DirectSPR) from dual-energy CT (DECT) and non-adapted clinical or adapted Hounsfield look-up table (HLUT) for two selected proton treatment fields of three patient cases. For the respective treatment field, relative water-equivalent range shifts in beam direction are illustrated in beam's eye view (IEC gantry coordinate system) with the corresponding (mean ± standard deviation).

Figure 6: Conversion from CT number to (A) stopping-power ratio (SPR) and (B) mass-density ratio (MDR) relative to water before and after HLUT refinement as clinically implemented in the treatment planning system XiO and RayStation at the University Proton Therapy Dresden, respectively.

Table 1: Clinical conversion from CT number to stopping-power ratio (SPR) before and after refinement of the Hounsfield look-up table (HLUT). The conversions from CT number to mass-density ratio (MDR) for the treatment planning system RayStation are provided as supplementary material.

Acknowledgments:

We thank in particular Julia Thiele and her team[||] for taking care of the DECT acquisition for treatment planning and during the course of treatment. Special thanks go to all patients, who consented to the retrospective evaluation of their data gathered for radiotherapy treatment planning. This work was funded by the National Center for Radiation Oncology (NCRO) within the project “Translation of dual-energy CT into application in particle therapy” and considered in the PhD thesis of Patrick Wohlfahrt [30].

Conflict of interest:

P. Wohlfahrt, S. Greilich and C. Richter received individual funding as lecturer from Siemens Healthineers (2018), which are not related to this research study. M. Krause received funding for her research projects from IBA (2016) and Merck KGaA (2014-2018 for pre-clinical study). E.G.C. Troost received funding for her research projects from the European Union (2018-2022). In addition, M. Krause and E.G.C. Troost received research funding from Merck KGaA (2018-2020 for clinical study), Medipan GmbH (2014-2018), Attomol GmbH (2019-2021), GA Generic Assays GmbH (2019-2021), BTU Cottbus-Senftenberg (2019-2021), Gesellschaft für medizinische und wissenschaftliche genetische Analysen (2019-2021), Lipotype GmbH (2019-2021) and PolyAn GmbH (2019-2021). For the present study, M. Krause and E.G.C. Troost confirm that none of the above-mentioned funding sources were involved in this study. OncoRay has an institutional research agreement with Siemens Healthineers in the field of DECT for particle therapy (2016-2020). Furthermore, OncoRay has an institutional agreement as reference center for dual-energy CT in radiotherapy as well as a software evaluation contract with Siemens Healthineers. For the present study, the authors received no financial support involved in the study design or materials used, nor in the collection, analysis and interpretation of data nor in the writing of the publication. The other authors report no conflict of interest.